

# NavBench: Probing Multimodal Large Language Models for Embodied Navigation

Yanyuan Qiao<sup>1</sup> Haodong Hong<sup>2,3</sup> Wenqi Lyu<sup>1</sup> Dong An<sup>4</sup> Siqi Zhang<sup>5</sup>  
Yutong Xie<sup>4</sup> Xinyu Wang<sup>1</sup> Qi Wu<sup>1,\*</sup>

<sup>1</sup>The University of Adelaide <sup>2</sup>The University of Queensland <sup>3</sup>CSIRO Data61

<sup>4</sup>Mohamed bin Zayed University of Artificial Intelligence <sup>5</sup>Tongji University

 Project Website

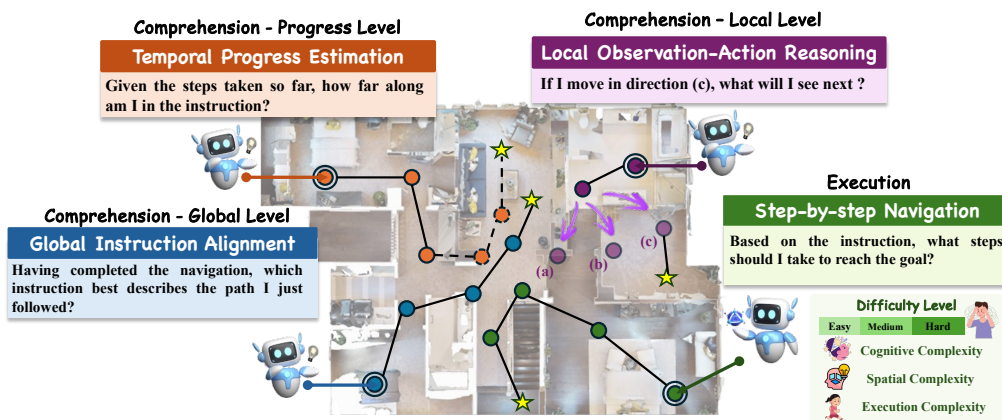


Figure 1: NavBench evaluates MLLMs across three comprehension tasks and a step-by-step execution task, assessing their ability to understand navigation behavior, track progress, reason about observation and action, and act accordingly. The step-by-step navigation is assessed from different difficulty levels, which is defined by cognitive, spatial, and execution complexity.

## Abstract

Multimodal Large Language Models (MLLMs) have demonstrated strong generalization in vision-language tasks, yet their ability to understand and act within embodied environments remains underexplored. We present NavBench, a benchmark to evaluate the embodied navigation capabilities of MLLMs under zero-shot settings. NavBench consists of two components: (1) navigation comprehension, assessed through three cognitively grounded tasks including global instruction alignment, temporal progress estimation, and local observation-action reasoning, covering 3,200 question-answer pairs; and (2) step-by-step execution in 432 episodes across 72 indoor scenes, stratified by spatial, cognitive, and execution complexity. To support real-world deployment, we introduce a pipeline that converts MLLMs’ outputs into robotic actions. We evaluate both proprietary and open-source models, finding that GPT-4o performs well across tasks, while lighter open-source models succeed in simpler cases. Results also show that models with higher comprehension scores tend to achieve better execution performance. Providing map-based context improves decision accuracy, especially in medium-difficulty scenarios. However, most models struggle with temporal understanding, particularly in estimating progress during navigation, which may pose a key challenge.

\*Corresponding author

# 1 Introduction

Multimodal Large Language Models (MLLMs) [1, 2, 3] have achieved impressive performance across a wide range of vision-language tasks, demonstrating strong cross-modal reasoning and zero-shot generalization. These models excel at answering visual questions [4], interpreting videos [5], and performing complex multimodal reasoning [6]. As their capabilities expand, a central question emerges: do these models truly understand how to act in the physical world, or are they simply adept at processing static inputs?

Recent work has begun to explore MLLMs’ potential in embodied tasks by evaluating their spatial reasoning in 3D environments [7, 8]. However, these tasks primarily focus on perception and passive scene understanding, without assessing the model’s ability to make decisions or take actions. In comparison, navigation is a core embodied task that involves interpreting natural language instructions, analyzing visual observations, and making a sequence of decisions to reach a goal. Although navigation plays a crucial role in real-world applications, it remains relatively underexplored in the context of MLLMs. Traditional embodied navigation benchmarks, such as Room-to-Room (R2R) [9] and ObjectNav [10], were developed prior to the emergence of foundation models. These benchmarks rely on task-specific supervision and often reduce evaluation to final success rates, providing limited insight into whether a model genuinely understands the navigation behavior. In many cases, an agent may reach the goal by exploiting dataset biases or learning shortcuts, without correctly grounding the instruction or following the intended path.

Similar to how humans acquire embodied skills by first understanding a task and then learning to execute it, evaluating the embodied capabilities of generalist MLLMs also requires examining two fundamental aspects. First, can the model comprehend what a navigation behavior represents, such as identifying the intent behind a completed trajectory? Second, can it act autonomously to complete a navigation task, making step-by-step decisions in unfamiliar environments? Furthermore, navigation tasks in real-world environments can vary significantly in difficulty due to differences in spatial layout, instruction complexity, and required decision-making steps. For example, navigating across multiple rooms with ambiguous instructions poses greater challenges than following simple step-by-step commands in a single hallway. However, most existing benchmarks treat all navigation episodes equally difficult, failing to capture this essential variation.

To fill these gaps, we introduce **NavBench**, a benchmark designed to systematically evaluate MLLMs in embodied navigation under zero-shot settings. NavBench decomposes the evaluation into two complementary components: *Navigation Comprehension*, which assesses whether a model understands and aligns with intended navigation behavior, and *Navigation Execution*, which evaluates the model’s ability to make accurate step-by-step decisions. To reflect real-world variability, NavBench incorporates a fine-grained difficulty classification based on spatial, cognitive, and execution complexity. In addition, it provides a deployable real-world navigation pipeline to bridge the gap between simulation and practical embodiment.

**First**, for navigation behavior comprehension, inspired by cognitive studies of human spatial reasoning [11], NavBench introduces three fine-grained evaluation tasks designed to assess distinct reasoning capabilities at three levels: global, progress, and local. It includes 3,200 question-answer pairs. Specifically, *Global Instruction Alignment* evaluates the model’s ability to match a given trajectory with the most appropriate instruction. The candidate instructions are designed with subtle semantic differences, such as variations in directional cues and landmark descriptions, to encourage genuine spatial reasoning. *Temporal Progress Estimation* measures temporal-contextual awareness by requiring the model to infer progress within multi-step instructions based on a partial trajectory. *Local Observation-Action Inference* evaluates the model’s ability to reason about the spatial consequences of individual actions by either predicting the future observation given an action or identifying the action that caused a visual transition. Together, these tasks provide a comprehensive framework for assessing global semantic reasoning, temporal understanding, and local spatial inference in navigation.

**Second**, NavBench introduces a fine-grained difficulty classification with three levels: easy, medium, and hard, based on cognitive, spatial, and execution complexity. This allows detailed analysis of models’ generalization and decision-making performance across varying levels of difficulty. The benchmark includes 432 navigation cases across 72 scenes.

**Finally**, to bridge the gap between simulator-based evaluation and real-world deployment, we design a practical navigation pipeline that connects MLLM outputs to executable actions on real robots. This

pipeline includes a waypoint selection module, an MLLM-based navigator, and a low-level controller, demonstrating the deployability of our framework in physical environments.

We evaluate both closed-source and open-source MLLMs on NavBench. While GPT-4o currently achieves the best overall performance, we observe that lightweight models such as Qwen2.5-VL-7B are capable of reliably completing easy navigation tasks. Notably, this trend is also reflected in our real-world deployment experiments, suggesting that NavBench may serve as a practical tool for analyzing the embodied capabilities of both general and resource-efficient MLLMs. Furthermore, our results suggest several notable trends: (1) comprehension and execution abilities appear to be closely related, (2) temporal reasoning may pose a persistent challenge for current models, and (3) compact open-source models can, under certain conditions, approach the performance of proprietary ones, indicating their potential utility in practical settings.

In summary, our main contributions are as follows: (1) We introduce *NavBench*, a benchmark for evaluating MLLMs in embodied navigation under zero-shot settings. (2) We decompose the evaluation into two components: *Navigation Comprehension*, with tasks targeting spatial, temporal, and local reasoning, and *Navigation Execution*, which assesses decision-making across difficulty levels. (3) We develop a deployment pipeline that maps MLLM outputs to real-world robot actions. (4) We perform a detailed evaluation and analysis of both closed-source and open-source MLLMs, uncovering trends in their reasoning and execution performance across embodied tasks.

## 2 Related Work

**Benchmarks for MLLMs** Recent progress in Multimodal Large Language Models (MLLMs) [1, 12, 13, 14, 15] has driven the development of benchmarks assessing visual understanding and cross-modal reasoning. Early efforts such as VQA [4], GQA [16], OK-VQA [17], and TextVQA [18] focus on specific tasks like factual or commonsense question answering. More recent benchmarks including MME [19], MMBench [20], MM-Vet [21], and MathVista [6] aim for broader coverage, evaluating perception and reasoning across diverse domains. However, these mainly target static tasks and do not reflect MLLMs’ ability to act in dynamic environments. To bridge this gap, some recent work has begun evaluating spatial reasoning in embodied settings. SpatialBench [7], ScanReason [22], and VSI-Bench [8] assess 3D spatial understanding using panoramas, semantic layouts, or textual scene descriptions. While insightful for embodied perception, they remain limited to passive tasks and do not assess decision-making or sequential interaction. In parallel, traditional embodied navigation benchmarks such as R2R [9], REVERIE [23], and ObjectNav [10] have long been used to test instruction-following agents. However, they were designed for fully supervised settings and mainly evaluate success rates without probing intermediate reasoning. Although REVERIE increases instruction abstraction, it retains similar path lengths and decision complexity, limiting its capacity to reveal behavioral differences. More recently, Wang *et al.* [24] proposed a fine-grained evaluation framework for instruction understanding in VLN via multiple-choice questions, offering interpretability beyond end-to-end metrics. Still, their setup is restricted to small supervised models and lacks real-world deployment and zero-shot inference. To the best of our knowledge, no existing benchmark offers a comprehensive evaluation of MLLMs in embodied navigation that jointly considers instruction understanding, sequential decision-making, difficulty stratification, and real-world transferability.

**Embodied Navigation** Embodied navigation tasks require an agent to reach a goal location within an environment, guided by a description such as an image [25, 26], object [10, 27], or natural language instruction [9, 28, 29]. Among these, language-guided navigation has attracted significant attention for its potential to facilitate intuitive human-robot interaction. Researchers have explored diverse instruction formats, including step-by-step [9, 30], dialog-based [31], and goal- or intention-oriented instructions [23, 32]. Traditional approaches train navigation policies using annotated datasets, incorporating modules to improve object relation understanding [33, 34, 35], vision-language alignment [36, 37, 38], memory [39, 40, 41], and spatial reasoning [42, 43, 44]. While effective on benchmarks, these methods often suffer from limited generalization due to dataset biases [45, 46, 47]. To mitigate this, recent work turns to MLLMs for zero-shot embodied navigation, leveraging their generalization abilities. Some use MLLMs to localize goal-relevant regions [48, 49, 50], while others employ prompt-based guidance for instruction following [51, 52, 53, 54]. These approaches reduce reliance on task-specific training but still lack fine-grained evaluation: most benchmarks focus solely on final success rates, offering limited insight into the model’s reasoning process. To address this, we

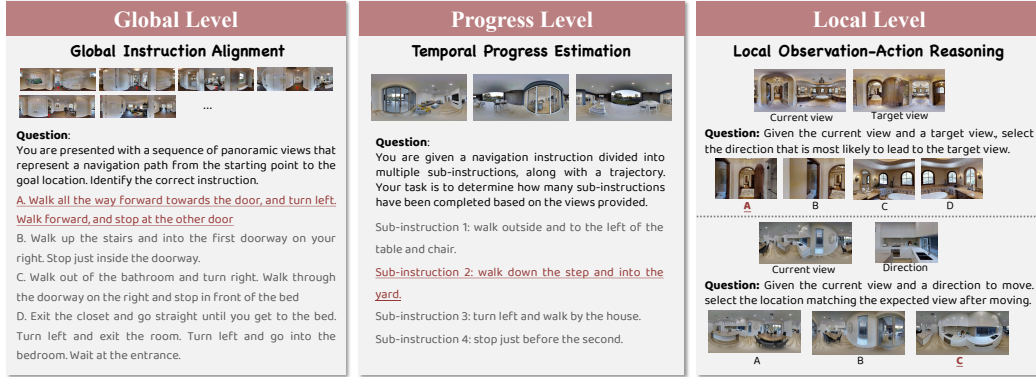


Figure 2: Illustration of the Navigation Comprehension task.

introduce NavBench, a benchmark that systematically evaluates both the reasoning and execution capabilities of MLLMs in embodied navigation.

### 3 Benchmark Design

#### 3.1 Task Formulation

We evaluate the navigation capabilities of MLLMs by decomposing the task into two core components: *Navigation Comprehension*, which assesses the understanding of navigation behavior, and *Navigation Execution*, which focuses on step-by-step decision making.

**Navigation Comprehension** It investigates whether the model can understand and reason about implicit navigation behaviors, including aligning instructions with trajectories, estimating progress along a plan, and predicting the spatial consequences of actions. These tasks span different reasoning levels (*global*, *progress*, and *local*) and serve as diagnostic probes for navigation understanding. Illustrations of the three comprehension tasks are shown in Figure 2<sup>2</sup>.

- **Global Level – Global Instruction Alignment:** Given a navigation trajectory and several candidate instructions, the model is required to determine which instruction aligns with the executed path. This task tests the model’s understanding of the overall intent and structural coherence of the navigation behavior.
- **Progress Level – Temporal Progress Estimation:** Provided with a partial trajectory and a list of segmented sub-instructions, the model must identify the sub-instruction that was most recently completed. This evaluates the model’s capacity to monitor task progress and comprehend the temporal structure of instructions.
- **Local Level – Local Observation-Action Reasoning:** To evaluate the model’s ability to reason about the spatial consequences of individual actions. We design two variants: (1) Future-Observation Prediction – the model observes the current view and an action, and selects the correct resulting view. (2) Future-Action Prediction – the model observes two consecutive views and must identify the action that caused the transition.

**Navigation Execution** It examines whether an MLLM can make accurate, step-by-step movement decisions in an embodied environment based on the current observation and instruction. We conduct this evaluation in a zero-shot setting [54] within the Matterport3D simulator [55], categorizing tasks into three difficulty levels (easy, medium, and hard) to assess performance. To ensure a fair and standardized evaluation protocol, we evaluate MLLMs via viewpoint selection rather than low-level action prediction (e.g., turning or moving forward). This abstraction, consistent with prior embodied navigation benchmarks [9, 23], allows us to focus on high-level semantic reasoning grounded in language and vision, while avoiding the confounding variability introduced by continuous control. It also facilitates zero-shot evaluation and comparability across different models. Notably, while our simulator setup centers on abstracted decision-making, Section 4 illustrates how this framework can be extended to real-world navigation by converting viewpoint selection into low-level control.

<sup>2</sup>The questions in the figure are slightly simplified for clarity and brevity.

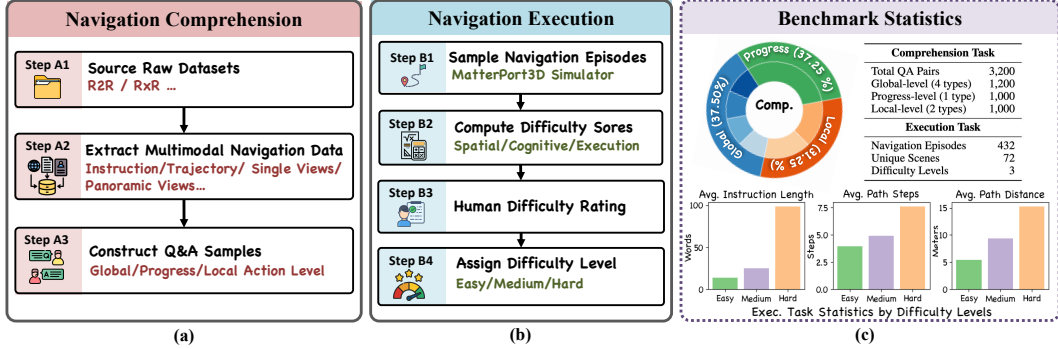


Figure 3: **NavBench construction pipeline and statistics.** (a) QA generation for comprehension tasks at global, progress, and local levels. (b) Execution pipeline combining automatic difficulty scoring and human ratings. (c) Benchmark statistics, including comprehension (comp.) task distribution, QA counts, and execution statistics (e.g., instruction length, steps, distance).

Specifically, at each step, the model receives the current panoramic observation, the natural language instruction, and a list of candidate navigable viewpoints. The model must select the next location to move to, thereby executing the instruction step-by-step until the goal is reached. Formally, at each step  $t$  of a navigation episode, the MLLM receives an instruction  $x = \{w_1, w_2, \dots, w_L\}$  of length  $L$ , a set of candidate navigable observation viewpoints  $O_t = \{o_t^1, o_t^2, \dots, o_t^N\}$ , and optional context  $C_t$  (such as navigation history or previous actions). The agent must select an action  $a_t$  corresponding to one of the navigable directions:

$$a_t = \text{MLLM}(x, O_t, C_t) \quad (1)$$

This decision process may involve reasoning about the instruction, interpreting the current view, leveraging prior context, and anticipating the result of each candidate action.

## 3.2 Dataset Construction

**Data Sources** NavBench is constructed by reorganizing and enriching fine-grained navigation data with multimodal observations to enable zero-shot evaluation of MLLMs. We start by collecting instruction-trajectory pairs from multiple embodied navigation benchmarks, including R2R [9], RxR [30], GEL-R2R [56], and FGR2R [57]. These datasets serve as annotation sources, but do not include the visual inputs needed for multimodal reasoning. To address this gap, we use the Matterport3D simulator to extract both panoramic and single-viewpoint RGB images aligned with navigation trajectories. The image extraction process involves traversing agent paths, sampling intermediate viewpoints, and rendering corresponding visual observations. All visual and textual data are then organized into a unified structure that supports multiple reasoning tasks and enables consistent QA generation across comprehension and execution settings. Figure 3 shows the overall benchmark construction pipeline.

**Statistics** We report statistics in Figure 3(c), including distribution of comprehension subtasks and coverage of scenes and episodes in execution. These statistics reflect the scale and diversity of the benchmark across reasoning levels and scenes.

### 3.2.1 Question-and-Answer Pairs Collection

We design three diagnostic tasks targeting global alignment, temporal progress estimation, and local spatial and action reasoning. In total, we collect 3,200 question-and-answer pairs to evaluate comprehension capacity in embodied navigation.

**Global Instruction Alignment** To evaluate MLLMs’ ability to align spatial trajectories with semantically consistent instructions, we construct a multiple-choice dataset comprising 1,200 examples. Each example consists of a panoramic trajectory and five candidate instructions, including one ground-truth and four distractors. The distractors are generated using four perturbation strategies: (1) *Basic*: random instructions sampled from unrelated trajectories, testing global relevance; (2) *Directional replacements*, where spatial terms (e.g., “left”, “north”) are substituted using POS tagging via NLTK, probing directional grounding; (3) *Object replacements*, where noun phrases are replaced with unrelated landmarks drawn from an external landmark-annotated dataset [56], evaluating object-trajectory

grounding; (4) *Shuffled segments*, where human-annotated sub-instructions [57] are permuted to disrupt temporal structure while preserving grammaticality. Each instruction set is randomly ordered and paired with a panoramic trajectory composed of viewpoint sequences and movement annotations. The design promotes multimodal spatial reasoning and reduces reliance on superficial cues.

**Progress Estimation** This task is designed to evaluate a model’s ability to perform temporal reasoning and monitor execution progress during navigation. Each full navigation instruction is segmented into a sequence of sub-instructions, and each sub-instruction is aligned with a corresponding portion of the agent’s trajectory. We leverage fine-grained annotations [57], which provide this alignment between individual sub-instructions and the associated panoramic viewpoints traversed during execution. To construct evaluation examples, we truncate the trajectory at intermediate points that mark the end of specific sub-instructions. The model is presented with the truncated panoramic trajectory along with the full list of sub-instructions, and is required to predict the index of the last completed one. To ensure data quality and minimize ambiguity, we filter the examples using a curated list of valid instruction-path pairs. In total, we collect 1,000 such examples for evaluation.

**Local Observation-Action Reasoning** We design two multiple-choice reasoning tasks to evaluate a model’s capacity for local spatial and action reasoning inference. Both tasks present ambiguous scenarios that require fine-grained visual discrimination and understanding of plausible transitions. In Future-Observation Prediction, the model receives a current view and an action, and must choose the correct resulting view from a set of candidates. In Future-Action Prediction, the model observes two consecutive views and selects the action that best explains the transition. For both tasks, distractors are carefully sampled from nearby observations or visually similar actions to ensure ambiguity and challenge. We collect 500 examples for each format, yielding a total of 1,000 samples. All questions are formatted as multiple-choice queries to ensure consistency across evaluation tasks.

### 3.2.2 Navigation Episodes Collection

We sample 432 navigation cases from 72 unique scenes in the Matterport3D simulator [55]. To systematically assess the difficulty of each case, we define a composite complexity score across three orthogonal dimensions: *spatial*, *cognitive*, and *execution* complexity. Each dimension is derived from structural properties of the environment or linguistic cues in the instruction, following the methodology inspired by [58, 59]. In addition, human evaluation is conducted to further support and validate the difficulty classification process.

**Spatial Complexity** It quantifies the geometric and topological challenges of a navigation trajectory. We consider four features: (1) total path length  $d$ , (2) standard deviation of turn angles  $\theta$ , (3) vertical range  $z$  as a proxy for elevation change, and (4) 2D spatial area  $A$  covered by the path. A binary indicator  $\mathbb{I}(z > 1.5)$  is included to capture significant elevation changes such as floor transitions. These features are computed from agent poses and scene connectivity data. The spatial complexity score is defined as:

$$\Phi_{\text{spatial}} = \alpha_1 \cdot \log(1 + d) + \alpha_2 \cdot \log(1 + \theta) + \alpha_3 \cdot \mathbb{I}(z > 1.5) + \alpha_4 \cdot \log(1 + A) \quad (2)$$

**Cognitive Complexity** It reflects the linguistic difficulty of navigation instructions. We extract five features using dependency parsing: (1) instruction length  $L$ , (2) number of verbs  $V$ , (3) number of spatial terms  $S$  (e.g., *left*, *upstairs*), (4) number of landmark mentions  $M$  (e.g., *kitchen*), and (5) number of subordinate clauses  $C$  (e.g., `relcl`, `advcl`). The cognitive complexity score is defined as:

$$\Phi_{\text{cognitive}} = \beta_1 \cdot \log(1 + L) + \beta_2 \cdot \log(1 + V) + \beta_3 \cdot \log(1 + S) + \beta_4 \cdot \log(1 + M) + \beta_5 \cdot C \quad (3)$$

**Execution Complexity** It measures the behavioral effort required to complete the navigation. We consider: (1) number of steps  $N$ , (2) number of turns  $T$ , (3) floor change indicator  $F$ , and (4) number of decision points  $D$ . The score is computed as:

$$\Phi_{\text{execution}} = \gamma_1 \cdot \log(1 + N) + \gamma_2 \cdot \log(1 + T) + \gamma_3 \cdot F + \gamma_4 \cdot D \quad (4)$$

**Normalization** Each raw complexity score  $\Phi$  is normalized to the range [1, 9] using a non-linear mapping:

$$\hat{\Phi} = \text{round} \left( 1 + 8 \cdot \frac{\log(1 + \Phi) - \log(1 + \Phi_{\min})}{\log(1 + \Phi_{\max}) - \log(1 + \Phi_{\min})}, 2 \right) \quad (5)$$

The weights  $\alpha$ ,  $\beta$ , and  $\gamma$  are empirically set to balance the contribution of each factor.

**Human Evaluation** To complement the automatic scoring, we conducted a human evaluation to validate our difficulty annotations. A group of annotators independently rated each case along the three defined dimensions, using a 1–9 scale with detailed guidelines aligned to our scoring criteria.

**Difficulty Categorization** Based on the final scores, each case is categorized into one of three levels, as illustrated in Figure 4:

- Easy (score 1–3): Short paths with simple instructions, few steps, minimal spatial reasoning, and clear landmarks.
- Medium (score 4–6): Instructions with moderate length, multiple landmarks or spatial phrases, and medium-length paths.
- Hard (score 7–9): Long trajectories guided by complex multi-step instructions, often involving floor transitions and multiple spatial references.

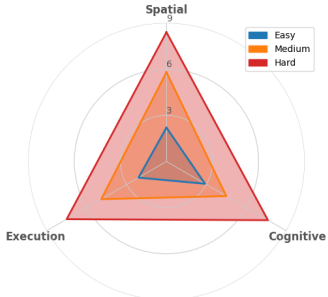


Figure 4: Radar chart of average complexity scores across cognitive, spatial, and execution dimensions for different difficulty levels.

## 4 Real-World Deployment Pipeline

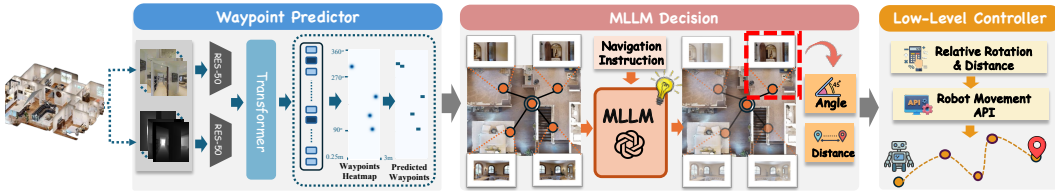


Figure 5: Overview of the real-world embodied navigation pipeline.

To demonstrate the real-world feasibility of MLLM-guided embodied navigation, we implement a modular pipeline that complements our benchmark evaluation, as illustrated in Figure 5. It consists of three modules: (1) a *Waypoint Predictor* that extracts RGB and depth inputs to generate candidate waypoints, (2) an *MLLM Decision Module* that selects the most goal-aligned waypoint, and (3) a *Low-Level Controller* that translates the selected waypoint into motion commands for execution on a physical robot. The system is deployed on a dual-arm mobile robot equipped with an RGB-D camera and evaluated in real indoor environments.

## 5 Evaluation on NavBench

### 5.1 Settings

**Models** We evaluate both proprietary and open-source MLLMs widely adopted in recent research. Proprietary models include GPT-4o and GPT-4o-mini. Open-source models include InternVL2.5-2B/8B [60], Qwen2.5-VL-3B/7B [61], LLaVA-OneVision-7B [62], and Llama3.2-Vision-11B [63].

**Implementation Details** Proprietary models are accessed via APIs, while open-source models are deployed using vLLM [64] and lmdeploy [65] on a single NVIDIA A6000 GPU (48GB). Simulator-based evaluations are conducted in the Matterport3D Simulator [55], built on high-resolution RGB-D scans of real indoor environments such as homes and offices. It provides realistic visual inputs and discrete agent movement within a 3D mesh, making it a standard testbed for embodied navigation. For real-world deployment, we integrate our pipeline with a dual-arm composite mobile robot equipped with an Intel RealSense D435 camera and a Water Drop 2 wheeled base. All physical experiments are conducted in a controlled indoor lab to assess robustness and feasibility.

**Evaluation Metrics** Our benchmark includes both multiple-choice reasoning and embodied navigation execution tasks. For multiple-choice questions, we follow standard practice [5] and use *Accuracy* as the primary metric, which measures whether the model selects the correct answer from a set of candidates based on the provided information. For execution tasks, we adopt standard metrics in embodied navigation [9, 30]. *Success Rate (SR)* measures the percentage of episodes where the target object is visible from the agent’s final viewpoint, defined as being within a 3-meter

Table 1: Performance comparison on **Navigation Comprehension** and **Execution**.

Model	Navigation Comprehension				Navigation Execution							
	Global	Progress	Local	Comp. Avg	Easy		Medium		Hard		Exec. Avg	
	Accuracy				SR	SPL	SR	SPL	SR	SPL		
Chance Level (Random)	19.33	25.4	29.34	24.65	16.41	9.57	7.17	3.72	7.33	4.99	8.19	
<b>VLN-Bench (tiny) Performance</b>												
† Human Level	88.33	79.00	85.00	84.11	91.67	88.68	87.50	81.53	75.00	65.17	81.59	
† GPT-4o	51.67	45.00	63.00	53.89	66.08	49.01	43.79	36.44	25.00	20.11	40.07	
† Qwen2.5-VL-7B	36.67	32.00	47.00	38.56	46.25	35.59	25.27	18.93	12.50	5.93	24.41	
<b>Closed Models</b>												
GPT-4o	<b>51.33</b>	<b>42.90</b>	<b>65.80</b>	<b>53.34</b>	<b>67.36</b>	<b>54.31</b>	<b>41.67</b>	<b>35.71</b>	<b>27.78</b>	<b>21.15</b>	<b>41.33</b>	
GPT-4o-mini	50.33	29.90	59.03	46.42	46.53	40.44	28.47	24.90	15.28	12.29	27.99	
<b>Open-Source Models</b>												
InternVL2.5-2B	<b>67.25</b>	23.40	11.25	33.97	25.69	25.29	6.94	6.68	7.64	5.86	13.02	
Qwen2.5-VL-3B	43.83	21.30	<b>50.63</b>	38.59	23.61	17.52	12.50	8.88	10.26	5.24	13.00	
InternVL2.5-8B	62.75	28.50	28.12	39.79	28.47	28.19	7.66	7.42	7.64	6.18	14.26	
Qwen2.5-VL-7B	57.58	<b>31.20</b>	47.00	<b>45.26</b>	<b>41.67</b>	<b>32.55</b>	<b>22.92</b>	<b>17.43</b>	10.42	5.67	<b>21.77</b>	
LLaVA-OneVision-7B	31.17	26.60	39.00	32.26	31.25	17.64	15.58	7.80	<b>15.02</b>	<b>7.84</b>	15.86	
Llama3.2-Vision-11B	36.00	23.40	29.10	14.75	27.08	25.90	10.42	9.19	10.02	7.60	15.04	

Note: **Dark teal** and **light teal** indicate the top-performing closed and open-source models per column.

† indicates results evaluated on the NavBench (tiny) subset.

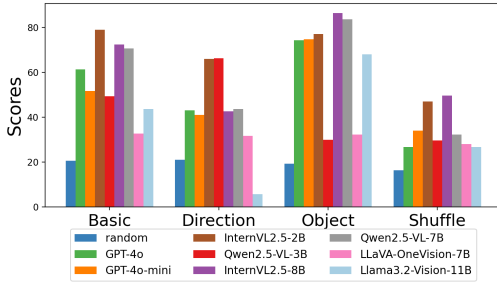


Figure 6: Model Performance under Different Instruction Perturbations.

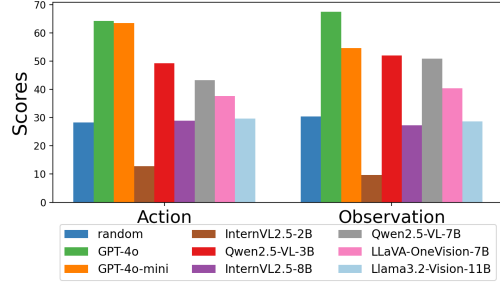


Figure 7: Model performance on Local Observation-Action Reasoning.

radius. *Success weighted by Path Length (SPL)* adjusts SR by path efficiency and is computed as  $SPL = \frac{1}{N} \sum_{i=1}^N S_i \cdot \frac{\ell_i}{\max(\ell_i, p_i)}$ , where  $N$  is the number of episodes,  $S_i \in \{0, 1\}$  indicates success,  $\ell_i$  is the shortest path, and  $p_i$  is the path length.

**VLN-Bench (tiny) Human Performance** To establish a human performance reference for VLN-Bench, we construct a compact evaluation subset named VLN-Bench (tiny) by randomly sampling a representative subset of tasks, inspired by the strategy in [8]. Annotating the entire dataset with human responses is impractical due to scale, so we select 120 multiple-choice questions for the Global Instruction Alignment task, 100 for Temporal Progress Estimation, 100 for Local Observation-Action Reasoning, and 72 navigation episodes for Execution Evaluation. All questions are in multiple-choice format with predefined correct answers. Human participants, who were volunteer students from our research institute with relevant backgrounds, independently completed each task. Their responses were automatically scored using the same metrics applied to model evaluation, including accuracy for comprehension tasks and SR/SPL for execution. This evaluation did not involve personal data collection or behavioral intervention and was conducted in accordance with institutional guidelines. In total, VLN-Bench (tiny) includes 392 human-evaluated questions and episodes.

## 5.2 Performance

We begin by examining the relationship between comprehension and execution. As shown in Table 1, model performance on comprehension and execution tasks is closely aligned. GPT-4o achieves the highest comprehension average (53.34%) and execution average (41.33%). Among open-source models, Qwen2.5-VL-7B performs best (45.26%, 21.77%), approaching GPT-4o-mini (46.42%, 27.99%) and demonstrating potential for deployment in real-world robotics. Turning to comprehension subtasks, InternVL2.5-2B achieves strong performance on Global Instruction Alignment (67.25%), even surpassing GPT-4o (51.33%). However, its accuracy drops sharply on

Table 2: Impact of map information on GPT-4o.

Diff.	Map	SR	SPL	Avg	Gain
Easy	✗	67.36	54.31	60.84	–
	✓	70.14	54.11	62.13	+1.29
Med.	✗	41.67	35.71	38.69	–
	✓	46.53	39.86	43.20	+4.51
Hard	✗	27.78	21.15	24.47	–
	✓	29.17	22.32	25.75	+1.28



Figure 8: Distribution of navigation error types identified from manual analysis.

more challenging reasoning tasks. In particular, Progress Estimation remains a consistent weakness across models: aside from GPT-4o (42.90%), all others perform poorly, highlighting current MLLMs’ limitations in temporal reasoning. We next analyze how models perform across navigation difficulty levels. Most open-source models can only reliably complete Easy episodes. While GPT-4o maintains relatively strong results across all difficulty levels, suggesting better generalization.

These findings suggest several overarching insights. First, comprehension and execution abilities are strongly linked. Second, temporal reasoning, particularly progress tracking, remains a major bottleneck. Third, compact open-source models like Qwen2.5-VL-7B can offer competitive performance with significantly lower resource requirements, making them promising for embodied applications.

### 5.3 Discussion

#### Breakdown of Distractor Types in Instruction Alignment

We further analyze performance on the Global Instruction Alignment task by breaking down results across four distractor types: *basic*, *direction*, *object*, and *shuffle*. As shown in Figure 6, most models handle the basic condition well, indicating their ability to reject unrelated instructions. However, performance under *direction* and *object* perturbations varies significantly across models, suggesting inconsistent grounding of spatial terms and landmarks. Notably, all models perform poorly under the *shuffle* condition, where sub-instructions are reordered but their content remains unchanged. This result is particularly revealing: despite the presence of the same entities and actions, altering the temporal structure makes the instruction much harder for models to interpret. The models’ failure in this setting highlights their limited ability to reason about temporal order within complex instructions. This finding aligns with the low scores observed in the Progress Estimation task, reinforcing that current MLLMs struggle with temporal understanding across both instruction-level and trajectory-level reasoning.

**Future-Action and Future-Observation Reasoning** We analyze performance on the Local Observation-Action Reasoning task, which includes two subtasks: Future-Action and Future-Observation Prediction. As shown in Figure 7, models show consistent performance across both, with GPT-4o clearly outperforming all others, consistent with its strong results in Navigation Execution. These subtasks reflect complementary reasoning skills. Future-Action Prediction tests whether a model can infer the spatial transition between two views, while Future-Observation Prediction requires anticipating how the environment changes after a given action. Both capabilities are critical for navigation, where agents should reason about cause and effect in spatial transitions.

**Effect of Map Information on Action Decisions** Although our benchmark evaluations assume no access to map information, reflecting real-world constraints, we investigate whether providing map connectivity can enhance action selection. Specifically, we follow the approach introduced in MapGPT, where topological relationships between explored nodes are encoded as text prompts. Using GPT-4o, we compare performance with and without map input across different difficulty levels. As shown in Table 2, the presence of map information consistently improves success rates, with the largest gain observed under medium difficulty, yielding an increase of 4.86 percentage points. This suggests that access to structured spatial context can facilitate better high-level reasoning and planning, especially in medium complexity settings where spatial ambiguity is more common.

**Error Analysis** We manually analyze 100 failed cases to understand model failures. Based on thought traces and action sequences, we identify four common error types: (a) *Incorrect Plan*: the plan misaligns with the instruction; (b) *Misaligned Action*: the plan is valid, but the chosen

movement does not follow it; (c) *Failure to Stop*: the agent overshoots the goal or stops early; and (d) *Hallucinated Movement*: the model selects a nonexistent location. The error distribution is shown in Figure 8. These patterns align with weaknesses in comprehension tasks. For example, type (c) reflects poor *Progress Estimation*. This suggests execution failures often stem from temporal and spatial reasoning limitations, reinforcing the diagnostic value of NavBench.

**Real-World Validation** To assess the feasibility of our real-world deployment pipeline, we conduct a pilot study in an indoor environment using GPT-4o and Qwen2.5-VL-7B, the top proprietary and open-source models from our benchmark. Each model is tested on 10 cases, achieving success rates of 60% and 40%, respectively. These results show that both can handle simple navigation tasks in real-world settings. Their success trends mirror execution performance in Table 1, where both models outperform others in their categories. This suggests that NavBench’s simulation-based evaluation reliably reflects real-world embodied performance.

## 6 Conclusion

This paper presents NavBench, a diagnostic benchmark designed to evaluate MLLMs in embodied navigation under zero-shot settings. It decomposes the evaluation into two components: Navigation Comprehension, which evaluates global instruction alignment, temporal progress estimation, and local observation-action reasoning through three cognitively grounded tasks, and Navigation Execution, which examines step-by-step decision-making across varying levels of difficulty. Additionally, we develop a pipeline for real-world deployment of MLLM-driven agents. Through evaluation and targeted analysis, NavBench reveals limitations in temporal understanding and action grounding that are not captured by standard success metrics. It also shows that lightweight open-source models can be effective in simpler navigation scenarios. We hope NavBench can serve as a useful resource for analyzing the embodied capabilities of MLLMs and supporting future work in this direction.

## References

- [1] Haotian Liu, Chunyuan Li, Qingyang Wu, and Yong Jae Lee. Visual instruction tuning. In *Advances in Neural Information Processing Systems*, volume 36, 2023.
- [2] Peng Wang, Shuai Bai, Sinan Tan, Shijie Wang, Zhihao Fan, Jinze Bai, Keqin Chen, Xuejing Liu, Jialin Wang, Wenbin Ge, Yang Fan, Kai Dang, Mengfei Du, Xuancheng Ren, Rui Men, Dayiheng Liu, Chang Zhou, Jingren Zhou, and Junyang Lin. Qwen2-vl: Enhancing vision-language model’s perception of the world at any resolution. *arXiv preprint arXiv:2409.12191*, 2024.
- [3] Gemini Team, Petko Georgiev, Ving Ian Lei, Ryan Burnell, Libin Bai, Anmol Gulati, Garrett Tanzer, Damien Vincent, Zhufeng Pan, Shibo Wang, et al. Gemini 1.5: Unlocking multimodal understanding across millions of tokens of context. *arXiv preprint arXiv:2403.05530*, 2024.
- [4] Yash Goyal, Tejas Khot, Douglas Summers-Stay, Dhruv Batra, and Devi Parikh. Making the v in vqa matter: Elevating the role of image understanding in visual question answering. In *Proceedings of the IEEE conference on computer vision and pattern recognition*, pages 6904–6913, 2017.
- [5] Chaoyou Fu, Yuhan Dai, Yondong Luo, Lei Li, Shuhuai Ren, Renrui Zhang, Zihan Wang, Chenyu Zhou, Yunhang Shen, Mengdan Zhang, Peixian Chen, Yanwei Li, Shaohui Lin, Sirui Zhao, Ke Li, Tong Xu, Xiawu Zheng, Enhong Chen, Rongrong Ji, and Xing Sun. Video-mme: The first-ever comprehensive evaluation benchmark of multi-modal llms in video analysis. *ArXiv*, abs/2405.21075, 2024.
- [6] Pan Lu, Hritik Bansal, Tony Xia, Jiacheng Liu, Chunyuan Li, Hannaneh Hajishirzi, Hao Cheng, Kai-Wei Chang, Michel Galley, and Jianfeng Gao. Mathvista: Evaluating mathematical reasoning of foundation models in visual contexts. *arXiv preprint arXiv:2310.02255*, 2023.
- [7] Wenxiao Cai et al. Spatialbot: Precise spatial understanding with vision language models. In *IEEE international conference on robotics and automation*, 2025.
- [8] Jihan Yang, Shusheng Yang, Anjali Gupta, Rilyn Han, Li Fei-Fei, and Saining Xie. Thinking in Space: How Multimodal Large Language Models See, Remember and Recall Spaces. In *IEEE/CVF Conference on Computer Vision and Pattern Recognition*, 2025.
- [9] Peter Anderson, Qi Wu, Damien Teney, Jake Bruce, Mark Johnson, Niko Sünderhauf, Ian D. Reid, Stephen Gould, and Anton van den Hengel. Vision-and-language navigation: Interpreting visually-grounded navigation instructions in real environments. In *CVPR*, pages 3674–3683, 2018.

- [10] Devendra Singh Chaplot, Dhiraj Prakashchand Gandhi, Abhinav Gupta, and Russ R Salakhutdinov. Object goal navigation using goal-oriented semantic exploration. *Advances in Neural Information Processing Systems*, 33:4247–4258, 2020.
- [11] Benjamin Kuipers. The spatial semantic hierarchy. *Artificial intelligence*, 119(1-2):191–233, 2000.
- [12] Zhe Chen, Jiannan Wu, Wenhai Wang, Weijie Su, Guo Chen, Sen Xing, Zhong Muyan, Qinglong Zhang, Xizhou Zhu, Lewei Lu, Bin Li, Ping Luo, Tong Lu, Yu Qiao, and Jifeng Dai. Intern vl: Scaling up vision foundation models and aligning for generic visual-linguistic tasks. *IEEE/CVF Conference on Computer Vision and Pattern Recognition*, pages 24185–24198, 2023.
- [13] Jean-Baptiste Alayrac, Jeff Donahue, Pauline Luc, Antoine Miech, Iain Barr, Yana Hasson, Karel Lenc, Arthur Mensch, Katie Millican, Malcolm Reynolds, Roman Ring, Eliza Rutherford, Serkan Cabi, Tengda Han, Zhitao Gong, Sina Samangooei, Marianne Monteiro, Jacob Menick, Sebastian Borgeaud, Andy Brock, Aida Nematzadeh, Sahand Sharifzadeh, Mikolaj Binkowski, Ricardo Barreira, Oriol Vinyals, Andrew Zisserman, and Karen Simonyan. Flamingo: a visual language model for few-shot learning. *ArXiv*, abs/2204.14198, 2022.
- [14] Jinze Bai, Shuai Bai, Shusheng Yang, Shijie Wang, Sinan Tan, Peng Wang, Junyang Lin, Chang Zhou, and Jingren Zhou. Qwen-vl: A frontier large vision-language model with versatile abilities. *ArXiv*, abs/2308.12966, 2023.
- [15] Haotian Liu, Chunyuan Li, Yuheng Li, and Yong Jae Lee. Improved baselines with visual instruction tuning. *IEEE/CVF Conference on Computer Vision and Pattern Recognition*, pages 26286–26296, 2023.
- [16] Drew A Hudson and Christopher D Manning. Gqa: A new dataset for real-world visual reasoning and compositional question answering. In *Proceedings of the IEEE/CVF conference on computer vision and pattern recognition*, pages 6700–6709, 2019.
- [17] Kenneth Marino, Mohammad Rastegari, Ali Farhadi, and Roozbeh Mottaghi. Ok-vqa: A visual question answering benchmark requiring external knowledge. In *Proceedings of the IEEE/cvf conference on computer vision and pattern recognition*, pages 3195–3204, 2019.
- [18] Amanpreet Singh, Vivek Natarajan, Meet Shah, Yu Jiang, Xinlei Chen, Dhruv Batra, Devi Parikh, and Marcus Rohrbach. Towards vqa models that can read. In *Proceedings of the IEEE/CVF conference on computer vision and pattern recognition*, pages 8317–8326, 2019.
- [19] Shukang Yin, Chaoyou Fu, Sirui Zhao, Ke Li, Xing Sun, Tong Xu, and Enhong Chen. A survey on multimodal large language models. *arXiv preprint arXiv:2306.13549*, 2023.
- [20] Yuan Liu, Haodong Duan, Yuanhan Zhang, Bo Li, Songyang Zhang, Wangbo Zhao, Yike Yuan, Jiaqi Wang, Conghui He, Ziwei Liu, et al. Mmbench: Is your multi-modal model an all-around player? In *European Conference on Computer Vision*, pages 216–233. Springer, 2025.
- [21] Weihao Yu, Zhengyuan Yang, Linjie Li, Jianfeng Wang, Kevin Lin, Zicheng Liu, Xinchao Wang, and Lijuan Wang. Mm-vet: Evaluating large multimodal models for integrated capabilities. *arXiv preprint arXiv:2308.02490*, 2023.
- [22] Chenming Zhu, Tai Wang, Wenwei Zhang, Kai Chen, and Xihui Liu. Scanreason: Empowering 3d visual grounding with reasoning capabilities. In *European Conference on Computer Vision*, 2024.
- [23] Yuankai Qi, Qi Wu, Peter Anderson, Xin Wang, William Yang Wang, Chunhua Shen, and Anton van den Hengel. REVERIE: remote embodied visual referring expression in real indoor environments. In *CVPR*, pages 9979–9988, 2020.
- [24] Zehao Wang, Minye Wu, Yixin Cao, Yubo Ma, Meiqi Chen, and Tinne Tuytelaars. Navigating the nuances: A fine-grained evaluation of vision-language navigation. *ArXiv*, abs/2409.17313, 2024.
- [25] Yuke Zhu, Roozbeh Mottaghi, Eric Kolve, Joseph J Lim, Abhinav Gupta, Li Fei-Fei, and Ali Farhadi. Target-driven visual navigation in indoor scenes using deep reinforcement learning. In *IEEE international conference on robotics and automation*, pages 3357–3364. IEEE, 2017.
- [26] Jacob Krantz, Stefan Lee, Jitendra Malik, Dhruv Batra, and Devendra Singh Chaplot. Instance-specific image goal navigation: Training embodied agents to find object instances. *arXiv preprint arXiv:2211.15876*, 2022.
- [27] Manolis Savva, Abhishek Kadian, Oleksandr Maksymets, Yili Zhao, Erik Wijmans, Bhavana Jain, Julian Straub, Jia Liu, Vladlen Koltun, Jitendra Malik, et al. Habitat: A platform for embodied ai research. In *Proceedings of the IEEE/CVF international conference on computer vision*, pages 9339–9347, 2019.

- [28] Shizhe Chen, Pierre-Louis Guhur, Cordelia Schmid, and Ivan Laptev. History aware multimodal transformer for vision-and-language navigation. In *Advances in Neural Information Processing Systems*, 2021.
- [29] Yue Zhang et al. Vision-and-language navigation today and tomorrow: A survey in the era of foundation models. *Transactions on Machine Learning Research*, 2024.
- [30] Alexander Ku, Peter Anderson, Roma Patel, Eugene Ie, and Jason Baldridge. Room-across-room: Multilingual vision-and-language navigation with dense spatiotemporal grounding. In *Proceedings of the Conference on Empirical Methods in Natural Language Processing*, pages 4392–4412, 2020.
- [31] Jesse Thomason, Michael Murray, Maya Cakmak, and Luke Zettlemoyer. Vision-and-dialog navigation. In *CoRL*, pages 394–406, 2019.
- [32] Hongcheng Wang, Andy Guan Hong Chen, Xiaoqi Li, Mingdong Wu, and Hao Dong. Find what you want: Learning demand-conditioned object attribute space for demand-driven navigation. In *Advances in Neural Information Processing Systems*, 2023.
- [33] Yuankai Qi, Zizheng Pan, Shengping Zhang, Anton van den Hengel, and Qi Wu. Object-and-action aware model for visual language navigation. In *European Conference on Computer Vision*, pages 303–317. Springer, 2020.
- [34] Yicong Hong, Cristian Rodriguez, Yuankai Qi, Qi Wu, and Stephen Gould. Language and visual entity relationship graph for agent navigation. *Advances in Neural Information Processing Systems*, 33:7685–7696, 2020.
- [35] Dong An, Yuankai Qi, Yan Huang, Qi Wu, Liang Wang, and Tieniu Tan. Neighbor-view enhanced model for vision and language navigation. In *Proceedings of the 29th ACM International Conference on Multimedia*, pages 5101–5109, 2021.
- [36] Weituo Hao, Chunyuan Li, Xiujun Li, Lawrence Carin, and Jianfeng Gao. Towards learning a generic agent for vision-and-language navigation via pre-training. In *Proceedings of the IEEE/CVF conference on computer vision and pattern recognition*, pages 13137–13146, 2020.
- [37] Pierre-Louis Guhur, Makarand Tapaswi, Shizhe Chen, Ivan Laptev, and Cordelia Schmid. Airbert: In-domain pretraining for vision-and-language navigation. In *Proceedings of the IEEE/CVF International Conference on Computer Vision*, pages 1634–1643, 2021.
- [38] Arjun Majumdar, Ayush Shrivastava, Stefan Lee, Peter Anderson, Devi Parikh, and Dhruv Batra. Improving vision-and-language navigation with image-text pairs from the web. In *Computer Vision—ECCV 2020: 16th European Conference, Glasgow, UK, August 23–28, 2020, Proceedings, Part VI 16*, pages 259–274. Springer, 2020.
- [39] Shizhe Chen, Pierre-Louis Guhur, Cordelia Schmid, and Ivan Laptev. History aware multimodal transformer for vision-and-language navigation. *Advances in neural information processing systems*, 34:5834–5847, 2021.
- [40] Yanyuan Qiao, Yuankai Qi, Yicong Hong, Zheng Yu, Peng Wang, and Qi Wu. Hop: History-and-order aware pre-training for vision-and-language navigation. In *Proceedings of the IEEE/CVF Conference on Computer Vision and Pattern Recognition*, pages 15418–15427, 2022.
- [41] Yanyuan Qiao, Yuankai Qi, Yicong Hong, Zheng Yu, Peng Wang, and Qi Wu. Hop+: History-enhanced and order-aware pre-training for vision-and-language navigation. *IEEE Transactions on Pattern Analysis and Machine Intelligence*, 45(7):8524–8537, 2023.
- [42] Dong An, Yuankai Qi, Yangguang Li, Yan Huang, Liang Wang, Tieniu Tan, and Jing Shao. Bevbort: Multimodal map pre-training for language-guided navigation. In *Proceedings of the IEEE/CVF International Conference on Computer Vision*, pages 2737–2748, 2023.
- [43] Rui Liu, Xiaohan Wang, Wenguan Wang, and Yi Yang. Bird’s-eye-view scene graph for vision-language navigation. In *Proceedings of the IEEE/CVF International Conference on Computer Vision*, pages 10968–10980, 2023.
- [44] Zihan Wang, Xiangyang Li, Jiahao Yang, Yeqi Liu, and Shuqiang Jiang. Gridmm: Grid memory map for vision-and-language navigation. In *Proceedings of the IEEE/CVF International Conference on Computer Vision*, pages 15625–15636, 2023.
- [45] Zun Wang, Jialu Li, Yicong Hong, Yi Wang, Qi Wu, Mohit Bansal, Stephen Gould, Hao Tan, and Yu Qiao. Scaling data generation in vision-and-language navigation. In *Proceedings of the IEEE/CVF International Conference on Computer Vision*, pages 12009–12020, 2023.

- [46] Aishwarya Kamath, Peter Anderson, Su Wang, Jing Yu Koh, Alexander Ku, Austin Waters, Yinfei Yang, Jason Baldridge, and Zarana Parekh. A new path: Scaling vision-and-language navigation with synthetic instructions and imitation learning. In *Proceedings of the IEEE/CVF Conference on Computer Vision and Pattern Recognition*, pages 10813–10823, 2023.
- [47] Jiazhao Zhang, Kunyu Wang, Rongtao Xu, Gengze Zhou, Yicong Hong, Xiaomeng Fang, Qi Wu, Zhizheng Zhang, and He Wang. Navid: Video-based vlm plans the next step for vision-and-language navigation. *arXiv preprint arXiv:2402.15852*, 2024.
- [48] Kaiwen Zhou, Kaizhi Zheng, Connor Pryor, Yilin Shen, Hongxia Jin, Lise Getoor, and Xin Eric Wang. Esc: Exploration with soft commonsense constraints for zero-shot object navigation. In *International Conference on Machine Learning*, pages 42829–42842. PMLR, 2023.
- [49] Samir Yitzhak Gadre, Mitchell Wortsman, Gabriel Ilharco, Ludwig Schmidt, and Shuran Song. Cows on pasture: Baselines and benchmarks for language-driven zero-shot object navigation. In *Proceedings of the IEEE/CVF Conference on Computer Vision and Pattern Recognition*, pages 23171–23181, 2023.
- [50] Naoki Yokoyama, Sehoon Ha, Dhruv Batra, Jiuguang Wang, and Bernadette Bucher. Vlfm: Vision-language frontier maps for zero-shot semantic navigation. In *IEEE international conference on robotics and automation*, pages 42–48. IEEE, 2024.
- [51] Yuxing Long, Wenzhe Cai, Hongcheng Wang, Guanqi Zhan, and Hao Dong. Instructnav: Zero-shot system for generic instruction navigation in unexplored environment. *arXiv preprint arXiv:2406.04882*, 2024.
- [52] Gengze Zhou, Yicong Hong, and Qi Wu. Navgpt: Explicit reasoning in vision-and-language navigation with large language models. In *Proceedings of the AAAI Conference on Artificial Intelligence*, volume 38, pages 7641–7649, 2024.
- [53] Yanyuan Qiao, Wenqi Lyu, Hui Wang, Zixu Wang, Zerui Li, Yuan Zhang, Mingkui Tan, and Qi Wu. Opennav: Exploring zero-shot vision-and-language navigation in continuous environment with open-source llms. *arXiv preprint arXiv:2409.18794*, 2024.
- [54] Jiaqi Chen, Bingqian Lin, Ran Xu, Zhenhua Chai, Xiaodan Liang, and Kwan-Yee Wong. Mapgpt: Map-guided prompting with adaptive path planning for vision-and-language navigation. In *Proceedings of the 62nd Annual Meeting of the Association for Computational Linguistics (Volume 1: Long Papers)*, pages 9796–9810, 2024.
- [55] Angel X. Chang, Angela Dai, Thomas A. Funkhouser, Maciej Halber, Matthias Nießner, Manolis Savva, Shuran Song, Andy Zeng, and Yinda Zhang. Matterport3d: Learning from RGB-D data in indoor environments. In *3DV*, pages 667–676, 2017.
- [56] Yibo Cui, Liang Xie, Yakun Zhang, Meishan Zhang, Ye Yan, and Erwei Yin. Grounded entity-landmark adaptive pre-training for vision-and-language navigation. *IEEE/CVF International Conference on Computer Vision*, pages 12009–12019, 2023.
- [57] Yicong Hong, Cristian Rodriguez, Qi Wu, and Stephen Gould. Sub-instruction aware vision-and-language navigation. In *Proceedings of the Conference on Empirical Methods in Natural Language Processing*, pages 3360–3376, 2020.
- [58] Xinyu Wang, Bohan Zhuang, and Qi Wu. Are large vision language models good game players? In *Proceedings of the International Conference on Learning Representations*, 2025.
- [59] Bosi Wen, Pei Ke, Xiaotao Gu, Lindong Wu, Hao Huang, Jinfeng Zhou, Wenchuang Li, Binxin Hu, Wendy Gao, Jiabin Xu, Yiming Liu, Jie Tang, Hongning Wang, and Minlie Huang. Benchmarking complex instruction-following with multiple constraints composition. *ArXiv*, abs/2407.03978, 2024.
- [60] Zhe Chen, Weiyun Wang, Yue Cao, Yangzhou Liu, Zhangwei Gao, Erfei Cui, Jinguo Zhu, Shenglong Ye, Hao Tian, Zhaoyang Liu, Lixin Gu, Xuehui Wang, Qingyun Li, Yiming Ren, Zixuan Chen, Jiapeng Luo, Jiahao Wang, Tan Jiang, Bo Wang, Conghui He, Botian Shi, Xingcheng Zhang, Han Lv, Yi Wang, Wenqi Shao, Pei Chu, Zhongying Tu, Tong He, Zhiyong Wu, Hui Deng, Jiaye Ge, Kaiming Chen, Min Dou, Lewei Lu, Xizhou Zhu, Tong Lu, Dahu Lin, Yunfeng Qiao, Jifeng Dai, and Wenhai Wang. Expanding performance boundaries of open-source multimodal models with model, data, and test-time scaling. *ArXiv*, abs/2412.05271, 2024.
- [61] Shuai Bai, Keqin Chen, Xuejing Liu, Jialin Wang, Wenbin Ge, Sibao Song, Kai Dang, Peng Wang, Shijie Wang, Jun Tang, Humen Zhong, Yuanzhi Zhu, Mingkun Yang, Zhaohai Li, Jianqiang Wan, Pengfei Wang, Wei Ding, Zheren Fu, Yiheng Xu, Jiabo Ye, Xi Zhang, Tianbao Xie, Zesen Cheng, Hang Zhang, Zhibo Yang, Haiyang Xu, and Junyang Lin. Qwen2.5-vl technical report. *ArXiv*, abs/2502.13923, 2025.

- [62] Bo Li, Yuanhan Zhang, Dong Guo, Renrui Zhang, Feng Li, Hao Zhang, Kaichen Zhang, Yanwei Li, Ziwei Liu, and Chunyuan Li. Llava-onevision: Easy visual task transfer. *arXiv preprint arXiv:2408.03326*, 2024.
- [63] Abhimanyu Dubey, Abhinav Jauhri, Abhinav Pandey, Abhishek Kadian, Ahmad Al-Dahle, Aiesha Letman, Akhil Mathur, Alan Schelten, Amy Yang, Angela Fan, et al. The llama 3 herd of models. *arXiv preprint arXiv:2407.21783*, 2024.
- [64] Woosuk Kwon, Zhuohan Li, Siyuan Zhuang, Ying Sheng, Lianmin Zheng, Cody Hao Yu, Joseph E. Gonzalez, Hao Zhang, and Ion Stoica. Efficient memory management for large language model serving with pagedattention. In *Proceedings of the ACM SIGOPS 29th Symposium on Operating Systems Principles*, 2023.
- [65] LMDeploy Contributors. Lmdeploy: A toolkit for compressing, deploying, and serving llm. <https://github.com/InternLM/lmdeploy>, 2023.